

NASA Technical Memorandum 81817

(NASA-TM-81817) EXPLORATORY PILOTED
SIMULATOR STUDY OF THE EFFECTS OF WINGLETS
ON HANDLING QUALITIES OF A REPRESENTATIVE
AGRICULTURAL AIRPLANE (NASA) 48 p
HC A03/MP A01

N80-28370

Unclass
28178

CSCL 01C G3/08

EXPLORATORY PILOTED SIMULATOR STUDY OF THE EFFECTS OF WINGLETS ON HANDLING QUALITIES OF A REPRESENTATIVE AGRICULTURAL AIRPLANE

MARILYN E. OGBURN AND PHILIP W. BROWN

APRIL 1980



**National Aeronautics and
Space Administration**

**Langley Research Center
Hampton, Virginia 23665**

EXPLORATORY PILOTTED SIMULATOR STUDY
OF THE EFFECTS OF WINGLETS
ON HANDLING QUALITIES OF A
REPRESENTATIVE AGRICULTURAL AIRPLANE

By

Marilyn E. Ogburn and Philip W. Brown
Langley Research Center

SUMMARY

An exploratory piloted simulator study has been conducted in order to evaluate the effects on handling qualities of adding winglets to a representative agricultural aircraft configuration during swath-run maneuvering. The aerodynamic data used in the simulation were based on low-speed wind-tunnel tests of a full-scale airplane and a subscale model. The simulation was conducted on the Langley General Purpose Simulator.

The results of the investigation showed that, for the task evaluated, the lateral-directional handling qualities of the airplane were greatly affected by the application of winglets and winglet cant angle. The airplane with winglets canted out 20° exhibited severely degraded lateral-directional handling qualities in comparison to the basic airplane. Excessive dihedral effect produced by the winglets contributed to the unsatisfactory lateral-directional behavior of the airplane. When the winglets were canted inward 10° , the dihedral effect was reduced and

the flying qualities of the configuration were markedly improved over those of the winglet-canted-out configuration. Also, the canted-in winglet configuration exhibited better handling characteristics than the basic configuration without winglets, indicating that proper tailoring of the winglet design may afford a potential benefit in the area of handling qualities. Due to the limited scope of this investigation, however, more research is needed in other areas of the flight envelope before specific recommendations on the use of winglets for agricultural aircraft can be made.

INTRODUCTION

Recent research by the National Aeronautics and Space Administration on agricultural aircraft has included an investigation of the effects of various wing tip modifications on the characteristics of wing tip vortex flow and the interaction of such flows with particles disbursed from the aircraft. In the swath run, the strong vortex flow field at the wing tip of a heavily loaded aircraft can have a predominant effect on swath width and uniformity of deposit. In some aerial applications, the entrainment of small chemical droplets in the vortex flow field can lead to serious drift problems, with large losses in efficiency of operation and productivity. The possibility of serious environmental damage adjacent to the working area is another serious problem when drift occurs. Results obtained from tests in the Langley Vortex Research Facility (reference 1) have shown that the use of winglets on agricultural aircraft may reduce this drift problem by diffusing the wing-tip

vortex and raising it to a higher position relative to the wing-mounted spray boom. These potential beneficial effects of winglets were shown to be relatively insensitive to changes in winglet cant angle, in the range between 20° canted out and 10° canted in.

On the basis of these promising results, a series of wind-tunnel tests of a full-scale aircraft and a small-scale model were performed, in order to determine the aerodynamic performance, stability, and control characteristics of a representative agricultural airplane with winglets. The wind-tunnel data for the aircraft with winglets (reference 2) showed moderate levels of improved performance only at high lift coefficients as would be expected (reference 3). However, the measured stability and control data indicated a potentially severe degradation in the lateral-directional handling qualities of the aircraft with winglets, due primarily to a large increase in the lateral stability derivative (dihedral effect).

An exploratory piloted simulation study was therefore conducted in order to determine the severity of the detrimental effects of winglets on the lateral-directional handling qualities of the aircraft and to develop potential solutions to any problems. The study was conducted on the Langley General Purpose Simulator, and a piloting task was designed to evaluate the effect of winglets on handling qualities during representative swath-run maneuvering. The aerodynamic data used in the simulation were based on the results of low-speed wind-tunnel tests of the full-scale aircraft and of a 1/10-scale model of the configuration.

SYMBOLS

All aerodynamic data and flight motions are referenced to the body system of axes shown in figure 1. The units for physical quantities used herein are presented in the International System of Units (SI) and U.S. Customary Units. The measurements and calculations were made in the U.S. Customary Units. Conversion factors for the two systems are given in reference 4.

a_n	normal acceleration, positive along negative Z body axis, g units ($1g = 9.8 \text{ m/sec}^2$)
a_y	lateral acceleration, positive along positive Y body axis, g units
b	wing span, m (ft)
C_D	drag coefficient, $\frac{\text{Aerodynamic drag force}}{\bar{q}S}$
$C_{D,t}$	total drag coefficient
C_L	lift coefficient, $\frac{\text{Aerodynamic lift force}}{\bar{q}S}$
$C_{L,t}$	total lift coefficient
C_l	rolling-moment coefficient about X body axis, $\frac{\text{Aerodynamic rolling moment}}{\bar{q}Sb}$
$C_{l,t}$	total rolling-moment coefficient
C_m	pitching-moment coefficient about Y body axis, $\frac{\text{Aerodynamic pitching moment}}{\bar{q}S\bar{c}}$

$C_{m,t}$	total pitching-moment coefficient
C_n	yawing-moment coefficient about Z body axis, <u>Aerodynamic yawing moment</u> $\bar{q}Sb$
$C_{n,t}$	total yawing-moment coefficient
C_T	thrust coefficient, $T/\rho n^2 D^4$
C_x	X-axis force coefficient along positive X body axis, <u>Aerodynamic X-axis force</u> $\bar{q}S$
$C_{x,t}$	total X-axis force coefficient
C_y	Y-axis force coefficient along positive Y body axis, <u>Aerodynamic Y-axis force</u> $\bar{q}S$
$C_{y,t}$	total Y-axis force coefficient
C_z	Z-axis force coefficient along positive Z body axis, <u>Aerodynamic Z-axis force</u> $\bar{q}S$
$C_{z,t}$	total Z-axis force coefficient
\bar{c}	wing mean aerodynamic chord, m (ft)
D	propeller diameter, ft
g	acceleration due to gravity, m/sec^2 (ft/sec^2)
h	altitude, m (ft)
I_x, I_y, I_z	moments of inertia about X, Y, and Z body axes, $kg-m^2$ ($slug-ft^2$)
I_{xz}	product of inertia with respect to X and Z body axes, $kg-m^2$ ($slug-ft^2$)
m	airplane mass, kg (slugs)
n	propeller rotational speed, $\frac{rev}{min}$

p	period, sec
p	airplane roll rate about X body axis, deg/sec or rad/sec
\dot{p}	airplane roll acceleration about X body axis, deg/sec ² or rad/sec ²
q	airplane pitch rate about Y body axis, deg/sec or rad/sec
\dot{q}	airplane pitch acceleration about Y body axis, deg/sec ² or rad/sec ²
\bar{q}	free-stream dynamic pressure, N/m ² (lb/ft ²)
r	yaw rate about Z body axis, deg/sec or rad/sec
\dot{r}	yaw acceleration about Z body axis, deg/sec ² or rad/sec ²
S	wing area, m ² (ft ²)
T	total instantaneous engine thrust, N (lb)
t	time, sec
$t_{1/2}$	time to damp to one-half amplitude, sec
u, v, w	components of airplane velocity along X, Y, and Z body axes, m/sec (ft/sec)
$\dot{u}, \dot{v}, \dot{w}$	airplane acceleration along X, Y, and Z body axes, m/sec ² (ft/sec ²)
V	airplane resultant velocity, m/sec (ft/sec)
X, Y, Z	airplane body axes (see figure 1)
α	angle of attack, deg
β	angle of sideslip, deg

δ_a aileron deflection, positive for left roll, deg
 δ_e elevator deflection, positive for pitch nose-down, deg
 δ_r rudder deflection, positive for left yaw, deg
 δ_T throttle position, fraction of maximum value
 δ_{w-} winglet cant angle from vertical, positive for outward cant, deg
 ζ damping ratio
 ρ atmospheric density, kg/m³ (slugs/ft³)
 Θ, ϕ Euler angles, deg
 τ time constant, sec

$$\begin{aligned}
 C_{L\delta_e} &= -\frac{\partial C_L}{\partial \delta_e} & C_{l_p} &= \frac{\partial C_l}{\partial \frac{pb}{2V}} & C_{l_r} &= \frac{\partial C_l}{\partial \frac{rb}{2V}} & C_{l\beta} &= \frac{\partial C_l}{\partial \beta} & C_{l\delta_a} &= \frac{\partial C_l}{\partial \delta_a} \\
 C_{l\delta_r} &= \frac{\partial C_l}{\partial \delta_r} & C_{m_q} &= \frac{\partial C_m}{\partial \frac{q\bar{c}}{2V}} & C_{m\delta_e} &= \frac{\partial C_m}{\partial \delta_e} & C_{n_p} &= \frac{\partial C_n}{\partial \frac{pb}{2V}} & C_{n_r} &= \frac{\partial C_n}{\partial \frac{rb}{2V}} \\
 C_{n\beta} &= \frac{\partial C_n}{\partial \beta} & C_{n\delta_a} &= \frac{\partial C_n}{\partial \delta_a} & C_{n\delta_r} &= \frac{\partial C_n}{\partial \delta_r} & C_{Y\beta} &= \frac{\partial C_Y}{\partial \beta} & C_{Y\delta_r} &= \frac{\partial C_Y}{\partial \delta_r}
 \end{aligned}$$

Subscripts:

DR .. dutch roll mode ____
 ge increment in variable produced by ground effect
 R roll mode
 S spiral mode
 δ_e increment in variable produced by elevator deflection

Abbreviations:

LCDP lateral control divergence parameter
 rpm revolutions per minute for engine

VFR visual flight rules
VLDS visual landing display system

DESCRIPTION OF AIRPLANE

A three-view sketch of the simulated airplane configuration, showing the two winglet configurations evaluated, is presented in figure 2, and the mass and geometric characteristics used in the simulation are listed in table I. The outwardly-canted winglet design ($\delta_w = 20^\circ$) was first proposed for the aircraft in an attempt to minimize the wake vortex problem discussed earlier. A second winglet cant angle, $\delta_w = -10^\circ$, was also evaluated after analysis indicated potentially degraded lateral-directional handling qualities for the configuration with canted-out winglets. As discussed in reference 2, the winglet planform and size were not optimized for this application; however, guidelines given in reference 5 were used to develop the configuration tested.

Conventional aerodynamic controls were simulated including conventional elevators for pitch control, deflection of wing-mounted ailerons for roll control, and rudder deflection for yaw control. Static aerodynamic data used in the simulation were obtained from the results of reference 2, dynamic derivatives were estimated using the methods of reference 6, and the effects of the propeller slipstream were neglected for this exploratory study. The effect of ground proximity on the aerodynamic data was also estimated.

All simulated flights were made for a center-of-gravity location of $0.30\bar{c}$, which is representative of an aft c.g. position for the simulated airplane.

DESCRIPTION OF SIMULATOR

Cockpit and Associated Equipment

A view of the cockpit of the General Purpose Fixed-Base Simulator is shown in figure 3. Force-feel characteristics for the control stick and rudder pedals are simulated by a programmable hydraulic servo system. Throttle controls for this study were located on the left side of the cockpit. A virtual image color visual display was provided for the piloting task. A sound system was used to provide aural cues relative to engine rpm and airspeed. —

Visual Display

The visual display utilized the Langley Visual Landing Display System (VLDS), which is displayed in color to the pilot through a refractive virtual image color display screen. The VLDS is a camera/model system which generates a visual out-the-window scene for the pilot of the simulated aircraft. The VLDS system consists of a 18.3 m-by-7.3 m (60 foot-by-24 foot) dual-scaled terrain model, a lampbank to illuminate the model, a three degree-of-freedom translation system to position the camera, and a three degree-of-freedom optical/rotational system mated to a color television camera. The VLDS provides non-composite television signals to an external simulator cockpit window display device to provide a field of view of 48 degrees horizontally and 36 degrees vertically. The optical/rotational system also employs a "sky plate" optical device to create the sky above the terrain scene and to provide for limited visibility conditions. Additional details pertaining to the VLDS and the general purpose simulator are given in references 7 and 8.

Computer Program and Equipment

The general purpose fixed-base simulator is driven by a real-time digital simulation system and a Control Data Cyber 175 computer. The dynamics of the evaluation airplane were calculated by using equations of motion with a fixed-interval (1/32 sec) numerical integration technique. The equations used aerodynamic data as a function of α in tabular form. These data were derived from results of low-speed static force tests of the full-scale aircraft and a one-tenth scale model, which were conducted at Langley (reference 2). The data included an angle-of-attack range from 0° to 20° , and all of the aerodynamic data presented herein are representative of a thrust coefficient (C_T) of 0.14. The equations of motion used are given in appendix A.

EVALUATION PROCEDURES

The results of the investigation were based on pilot comments and time-history records of airplane motions, controls, and the airplane flight path over the ground for the various maneuvers performed. The Cooper-Harper handling qualities rating scale (figure 4) and pilot comments were used to evaluate each configuration flown (reference 9). Most of the evaluations were performed by a NASA research test pilot who had recently completed training at an agricultural aircraft pilot school and had limited piloting experience in several different agricultural aircraft.

Task Description

A sketch which describes the piloting task used to evaluate the handling qualities of the aircraft is shown in figure 5. The task was designed to test the handling qualities of the aircraft in a manner which would be applicable to a realistic aircraft requirement. In this case, the straightforward task of maintaining wings level along a straight track in simulation of the unobstructed swath run was sufficient to reveal the relative handling qualities of the configurations studied.

The section of the VLDS terrain display used for the task (figure 6) includes one wide runway and its associated parallel taxiway. This taxiway centerline was the reference track. Lighting of the VLDS provided a day VFR scene with visibility of at least 5 miles. The task began with the aircraft positioned 610 meters (2,000 ft) from the runway edge at an altitude of 46 meters (150 ft) and trimmed for straight and level flight at 54 m/sec (120 mph). The pilot was required to approach the runway, dive down, and fly the complete length of the runway directly above the centerline, with fixed throttle position, at low altitude (about 3 meters). Lateral track corrections were made by wings-level sideslips which generated a sideforce, accelerating the airplane back toward the centerline. Pilot loop closure on lateral track error was made primarily by means of rudder inputs. Ailerons were used in response to bank angle errors which resulted from the rudder inputs. The pilot attempted to maximize lateral tracking performance while simultaneously holding the wings level and smoothly controlling attitude. Although no

external disturbances (such as turbulence or random lateral step offsets) were simulated, enough track, bank and altitude errors were induced by piloting to create a high workload task.

Once the aircraft reached the far end of the runway the run was terminated. The next run began from the same initial conditions; no turns were made between runs.

Evaluation of Handling Qualities

In evaluating the simulated airplane, numerous runs were made in the task. Sufficient flights were made to ensure that the pilot's "learning curve" was reasonably well established before drawing any conclusions on evaluation results. Evaluation of handling qualities was based on Cooper-Harper pilot ratings and pilot/vehicle performance.

DISCUSSION OF STABILITY AND CONTROL CHARACTERISTICS

To provide a foundation for the analysis and interpretation of the simulation results which follow, selected aerodynamic stability and control characteristics of the simulated aircraft configuration are presented and discussed in this section. The aerodynamic data for conditions in the swath run task are listed in table II, and the representation of these data in the equations of motion is discussed in appendix A.

Longitudinal Characteristics

The lift characteristics of the simulated configuration as noted during wind-tunnel tests were that the basic aircraft experienced a break in the lift curve at an angle of attack of about 15° , and another

break occurred at higher angles of attack (see figure 7(a)). As indicated by the lift data, the aircraft experiences an increase in lift with the addition of winglets. The longitudinal stability of the airplane was not significantly changed by the addition of winglets, as indicated by the pitching moment data (see figure 7(b)).

Lateral-Directional Characteristics

The static lateral-directional stability characteristics for the basic aircraft and each of the two winglet configurations are shown in figure 8. Figure 8(a) shows the static directional stability derivative, $C_{n\beta}$; figure 8(b) shows the lateral stability or effective dihedral derivative, $C_{l\beta}$, and the side-force derivative, $C_{Y\beta}$, is shown in figure 8(c), all as a function of angle of attack. At each angle of attack, each derivative was computed based on aerodynamic data at $\beta = +10^\circ$.

The data show that $C_{n\beta}$ remains positive (stable) for all three configurations through the range of angle of attack used in the performance of the swath run handling qualities evaluation task. However, some degradation in directional stability is indicated for $\delta_w = -10^\circ$ in comparison to the basic aircraft, and this degradation is more pronounced for $\delta_w = +20^\circ$. The plot of $C_{l\beta}$ against α (figure 8(b)) is of particular importance, since this plot shows that for $\delta_w = +20^\circ$, the winglets increased the positive effective dihedral ($-C_{l\beta}$) of the aircraft by a factor of about 3 for the angle-of-attack range of the swath run.

For $\delta_w = -10^\circ$, the increase in $-C_{l\beta}$ from the basic configuration was much less than for $\delta_w = +20^\circ$. This particular result was not unexpected, because of considerations which are illustrated in figure 9.

This figure shows the configuration with $\delta_w = 20^\circ$ and two geometric changes which might be used to reduce the effective dihedral. One change is to simply introduce negative geometric dihedral (anhedral) into the wings by lowering the wing tips. However, a calculation of the amount of wing dihedral angle change required in order for winglets with $\delta_w = +20^\circ$ to be added while maintaining the original effective dihedral of the basic aircraft shows that 12° of wing anhedral is required. As illustrated in figure 9, this method would result in probable wing tip contact with the ground during normal operations and is unacceptable. Another way of reducing dihedral effect for a configuration with winglets is to cant the winglets inward. This reduces the effective dihedral because under sideslipped conditions the force component normal to the winglet surface will be directed along a line which passes much closer to the center of gravity of the aircraft.

Another static derivative which is sensitive to winglets and winglet cant angle is C_{y_β} , which is plotted for each wing-tip configuration in figure 8(c). It is evident that the addition of the outwardly-canted winglets ($\delta_w = +20^\circ$) to the basic aircraft doubled the values of $-C_{y_\beta}$. There is also a substantial increase in $-C_{y_\beta}$ with the winglets canted inward ($\delta_w = -10^\circ$). The significance of this result in terms of its effect on the handling qualities of the subject aircraft will be described in a later section.

The dynamic lateral-directional stability characteristics of the airplane were calculated on the basis of three degree-of-freedom linearized lateral-directional equations and the aerodynamic data of

table II. The results of the calculations for the three wing-tip configurations are presented in table III. Data are shown for the Dutch roll, spiral, and roll modes of motion for the 1-g trim condition at the operating speed of the aircraft for the swath run. The data indicate that all the modes are stable. Both the degradation in directional stability as well as the increase in dihedral effect with winglets contributed to a slight decrease in Dutch roll damping. The Dutch roll damping is closer to that of the basic aircraft when the winglets are canted inward 10° . Some of the predominant effects that these stability characteristics have on the lateral-directional control characteristics of the aircraft will be discussed in the following section.

Lateral-Directional Control

The extent of the degradation in handling qualities of the aircraft due to the addition of winglets could not be adequately understood until a piloted evaluation could take place. However, an examination of some important stability and control parameters gave the first indication of potential problem areas. The lateral control divergence parameter (LCDP) is often used to appraise roll-control effectiveness. This parameter is defined as:

$$LCDP = C_{n_\beta} - C_{l_\beta} \frac{C_{n_{\delta a}}}{C_{l_{\delta a}}}$$

Positive values of this parameter indicate normal roll response (i.e., right roll control results in a right roll). When the LCDP is near zero, the roll response is weak and oscillatory, and negative values indicate

reversed response. When reversed response is encountered, a right roll control input results in a left roll (i.e., roll reversal). Low values of LCDP can result when the effective dihedral ($-C_{l\beta}$) is large and adverse yaw from aileron deflection ($C_{n\delta_a} > 0$) is present. The data of figure 10 show that the basic aircraft has positive values of LCDP for the swath run and would therefore be expected to have satisfactory levels of proper roll response with aileron deflection. The aircraft with winglets canted inward, $\delta_w = -10^\circ$, would also be expected to exhibit proper, though somewhat weakened roll response. With the winglets canted outward ($\delta_w = +20^\circ$), however, the ailerons are shown to be almost completely ineffective in rolling the aircraft, with a roll reversal indicated at about $\alpha = 4^\circ$. Deflection of the control stick for aileron control in the swath run would produce reversed or very weak roll response.

HANDLING QUALITIES EVALUATION RESULTS

Pilot-vehicle performance above the threshold of controllability lies on a continuous scale ranging from inadequate through adequate and desirable. Each category constitutes a line segment on this scale rather than a discrete point. For the swath run task, the desirable performance end of the spectrum would be characterized by only small amplitude track deviations and small, quick corrections to reacquire the reference line. Adequate performance would be typified by a larger range of deviations and slower corrective responses until reaching limits judged to be boundary conditions of this category. For this evaluation, the boundaries of these categories were assessed qualitatively by the

simulator pilot by observing the visual display.

Results for the Basic Airplane

The basic airplane was given a Cooper-Harper rating of 4 (see figure 4) and exhibited several minor deficiencies. Figure 11 shows an overhead view of a typical ground track for the basic airplane. The figure illustrates the length of the taxiway and its centerline (1372 m), which represents about 25 seconds of flying time. An expanded scale for the taxiway's width is used as an aid in visualizing the airplane ground track deviations from the centerline reference track. The pilot-vehicle performance for the basic airplane could be placed near the boundary between the "adequate" and "desirable" ranges on the continuous scale described above. Warranted improvements in the airplane would allow more expeditious corrections to the reference line and smaller amplitude deviations. The ability to generate more sideforce for a given sideslip angle would have improved the performance of this configuration so long as the bank control task did not correspondingly increase in difficulty.

The handling qualities of the basic airplane were considered representative of the behavior of agricultural airplanes and a reasonable baseline.

Results for the Winglets Canted Out 20°

The configuration with $\delta_w = 20^\circ$ was given a Cooper-Harper rating of 7, if the flight was maintained within relatively small sideslip angles ($\pm 10^\circ$). For larger sideslip angles, this configuration would sometimes roll off suddenly, rapidly, and uncontrollably, crashing

immediately. Such uncontrollable roll-offs occurred during about one-tenth of the runs. Figure 12 shows a typical track for this configuration. In addition to the very poor and sometimes divergent tracking performance, bank angle control was very poor. Altitude control suffered as a consequence of high sideslip excursions (causing high drag) and the high degree of pilot attention required to control ground track and bank angle.

These results were not unexpected, considering the previously—discussed aerodynamic lateral-directional stability and control characteristics of the aircraft. The large increase in dihedral effect due to the winglets, in combination with the decrease in directional stability, resulted in an easily excited Dutch roll mode. The simulated aircraft thus experienced excessive rolling motions following the rudder inputs. In addition, the ailerons, which could normally be used to counteract any unwanted rolling motion, were rendered almost useless by the presence of adverse yaw due to aileron deflection ($C_{n\delta_a} > 0$) and the large positive dihedral effect.

The canted-out winglet configuration also significantly increased $-C_{y\beta}$, which is desirable for use in ground track corrections. This potential benefit was negated by the excessive rolling moments generated by the winglets. The pilot was able to achieve adequate performance with a control technique which required an intolerable workload level; the pilot used no aileron inputs but only very high frequency rudder activity for control.

Results for the Winglets Canted in 10°

This configuration was given a Cooper-Harper rating of 3. Figure 13 shows a typical ground track for this configuration along with tracks for the basic and $\delta_w = 20^\circ$ cases. The results indicate a definite improvement in pilot/vehicle performance relative to the results obtained with outwardly-canted winglets and for the basic aircraft. The pilot's workload in performing the swath run task was comparable to that of the basic aircraft, and the overall handling qualities were considered to be better than those of the basic aircraft.

The improvement in handling qualities of the aircraft with inwardly-canted winglets over the basic aircraft was due in part to the increase in $-C_{y\beta}$. The high side forces generated by the winglets when the aircraft was sideslipped were beneficial for making lateral corrections. An even greater increase in $-C_{y\beta}$ was obtained when the winglets were canted out, but this potential benefit was negated by the fact that when the aircraft was sideslipped, excessive rolling motions and bank-angle divergences occurred. In summary, of the three wing-tip configurations studied, the aircraft with winglets canted inward 10° was judged to have the best handling qualities in the swath run task.

INTERPRETATION OF RESULTS

The fidelity of the simulation in representing an actual agricultural aircraft was evaluated by having a pilot with agricultural aircraft experience fly the simulator. The simulation was validated to the extent that the baseline aircraft characteristics were considered to be generally representative of agricultural aircraft. It should be

recognized, however, that the present study was limited in terms of simulator hardware and software, and these limitations should be kept in mind when applying the results and conclusions of this study. Some factors which introduced uncertainties in the simulation are (listed in order of their estimated importance):

- ① Simulation was fixed base.- Pilot loop closures might have been different if sideforce and roll acceleration cues had been available.
- ② Visual cues were limited.- Lack of peripheral vision could substantially affect pilot performance.
- ③ Limited validation of simulation.- The simulator was validated by having a pilot with agricultural airplane experience fly it and judge it to be generally representative of this type of airplane. A more credible simulation would be matched to actual flight data.
- ④ Lack of atmospheric disturbances.- No turbulence or wind inputs were used in the simulation. This was considered to be relatively unimportant because of the requirement for low wind conditions for many agricultural airplane missions.

In addition, the present study was limited in scope, being limited to only one area of the operational flight envelope, and only one task was used in the handling qualities evaluation.

SUMMARY OF RESULTS

An exploratory piloted simulator investigation has been conducted to evaluate the effect of winglets on the handling qualities of a representative agricultural airplane during swath run maneuvering. The

following major results were derived from this study:

1. Lateral-directional handling qualities may be greatly affected by the application of winglets to this class of aircraft.
2. Winglet cant angle can be used to vary the level of dihedral effect and lateral-directional handling qualities.
3. Proper tailoring of the winglet design may afford a potential benefit in the area of handling qualities due to increased side force generation for making lateral corrections in the swath run.
4. Stability, control, and handling qualities evaluations are needed in other areas of the flight envelope, particularly at high angles of attack (e.g., stall behavior), before specific recommendations on the use of winglets for agricultural aircraft can be made.

REFERENCES

1. Jordan, Frank L.; McLemore, H. Clyde; and Bragg, Michael B.:
"Status of Aerial Applications Research in the Langley Vortex Facility and the Langley Full-Scale Wind Tunnel." NASA TM 78760, 1978.
2. Johnson, Joseph L., Jr.; McLemore, H. Clyde; White, Richard; and Jordan, Frank L., Jr.: "Full-Scale Wind-Tunnel Investigation of an Ayres S2R-800 Thrush Agricultural Airplane." Society of Automotive Engineers, No. 790618, 1979.
3. Flechner, Stuart G.; and Jacobs, Peter F.: "Experimental Results of Winglets on First, Second, and Third Generation Jet Transports." NASA TM-72674, 1978.

4. Mechtly, E. A.: "The International System of Units - Physical Constants and Conversion Factors" (Second Revision). NASA SP-7012, 1973.
5. Whitcomb, Richard T.: "A Design Approach and Selected High Subsonic Speed Wind-Tunnel Results for Wing Tip Mounted Winglets." NASA TND-8260, 1976.
6. Hoak, E. E.; et al.: "USAF Stability and Control DATCOM," Air Force Flight Dynamics Lab, WPAFB, OH, February 1972.
7. Copeland, James L. (ed.): "Research through Simulation." NASA NF-125, 1979.
8. Rollins, John D.: "Description and Performance of the Langley Visual Landing Display System." NASA TM-78742, 1978.
9. Cooper, George E.; and Harper, Robert P., Jr.: "The Use of Pilot Rating in the Evaluation of Aircraft Handling Qualities." NASA TN D-5153, 1969.

APPENDIX A

DESCRIPTION OF EQUATIONS AND DATA EMPLOYED IN SIMULATION

Equations of Motion

The equations used to describe the motions of the airplane were non-linear, six-degree-of-freedom, rigid-body equations referenced to a body-fixed axis system shown in figure 1 and are given as follows:

Forces:

$$\dot{u} = rv - qw - g \sin \Theta + \frac{\bar{q}S}{m} C_{X,t} + \frac{T}{m}$$

$$\dot{v} = \underline{pw} - ru + g \cos \Theta \sin \phi + \frac{\bar{q}S}{m} C_{Y,t}$$

$$\dot{w} = qu - pv + g \cos \Theta \cos \phi + \frac{\bar{q}S}{m} C_{Z,t}$$

Moments:

$$\dot{p} = \frac{I_Y - I_Z}{I_X} qr + \frac{I_{XZ}}{I_X} (\dot{r} + pq) + \frac{\bar{q}Sb}{I_X} C_{l,t}$$

$$\dot{q} = \frac{I_Z - I_X}{I_Y} pr + \frac{I_{XZ}}{I_Y} (r^2 - p^2) + \frac{\bar{q}S\bar{c}}{I_Y} C_{m,t}$$

$$\dot{r} = \frac{I_X - I_Y}{I_Z} pq + \frac{I_{XZ}}{I_Z} (\dot{p} - qr) + \frac{\bar{q}Sb}{I_Z} C_{n,t}$$

where the total aerodynamic coefficients $C_{X,t}$, $C_{Z,t}$, $C_{m,t}$, $C_{Y,t}$, $C_{n,t}$, and $C_{l,t}$ are defined in the next section. Euler angles were computed by using quaternions to allow continuity of attitude motions.

Auxiliary equations included:

$$\alpha = \tan^{-1} \left(\frac{w}{u} \right)$$

$$\beta = \sin^{-1} \left(\frac{v}{V} \right)$$

$$V = \sqrt{u^2 + v^2 + w^2}$$

$$a_n = \frac{qu - pv + g \cos \theta \cos \phi - \dot{w}}{g}$$

$$a_y = \frac{-pw + ru - g \cos \theta \sin \phi + \dot{v}}{g}$$

Aerodynamic Data

The aerodynamic data used in the simulation were derived from low-speed wind-tunnel tests of the full-scale aircraft and of a 1/10-scale model of the configuration at the NASA Langley Research Center. The static aerodynamics and dynamic data were input in tabular form as a function of angle of attack over the range $0 \leq \alpha \leq 20^\circ$. Total coefficient equations were used to sum the various aerodynamic contributions to a given force or moment coefficient as follows.

For the X- and Z-axis force coefficients:

$$C_{X,t} = -C_{D,t} \cos \alpha + C_{L,t} \sin \alpha$$

$$C_{Z,t} = -C_{D,t} \sin \alpha - C_{L,t} \cos \alpha$$

where

$$C_{L,t} = C_L(\alpha, \delta_w) + C_{L_{\delta_e}}(\alpha) \delta_e + \Delta C_{L,ge}(C_{L,h})$$

$$C_{D,t} = C_D(\alpha, \delta_w) + \Delta C_{D,\delta_e}(\alpha, \delta_e) + \Delta C_{D,ge}(C_{D,h})$$

For the pitching-moment coefficient:

$$C_{m,t} = C_m(\alpha) + C_{m_{\delta_e}}(\alpha) \delta_e + C_{m_q}(\text{rpm}) \frac{\bar{c}q}{2V} + \Delta C_{m,ge}(C_{m,h})$$

For the Y-axis force coefficient:

$$C_{Y,t} = C_{Y_{\delta_r}}(\alpha) \delta_r + C_{Y_{\beta}}(\alpha, \delta_w) \beta$$

For the yawing-moment coefficient:

$$C_{n,t} = C_{n_{\delta_r}}(\alpha) \delta_r + C_{n_{\delta_a}}(\alpha, \delta_w) \delta_a + C_{n_r}(\alpha) \frac{rb}{2V} + C_{n_p}(\alpha) \frac{pb}{2V} \\ + C_{n_{\beta}}(\alpha, \delta_w) \beta$$

For the rolling-moment coefficient:

$$C_{l,t} = C_{l_{\delta_a}}(\alpha, \delta_w) \delta_a + C_{l_{\delta_r}}(\alpha) \delta_r + C_{l_p}(\alpha) \frac{pb}{2V} + C_{l_r}(\alpha, \delta_w) \\ \frac{rb}{2V} + C_{l_{\beta}}(\alpha, \delta_w) \beta$$

The aerodynamic coefficients contained in the preceding coefficient equations are presented for trim conditions at the operating speed for the swath run. The aerodynamic moment coefficients are referenced to a center-of-gravity location of 0.30 \bar{c} .

Engine Simulation

Presented in table IV are thrust values as a function of velocity and engine rpm, with engine rpm as a function of throttle position.

TABLE I.- MASS AND DIMENSIONAL CHARACTERISTICS
USED IN SIMULATION

Weight, N (lb)-----	34696	(7800)
Moments of inertia, kg-m ² (slug-ft ²):		
Basic aircraft		
I _X -----	6957	(5131)
I _Y -----	7572	(5585)
I _Z -----	13996	(10323)
I _{XZ} -----	66	(49)
Aircraft with winglets		
I _X -----	6995	(5159)
I _Y -----	7572	(5585)
I _Z -----	14034	(10351)
I _{XZ} -----	66	(49)
Wing dimensions:		
Span, m (ft)-----	13.53	(44.4)
Area, m ² (ft ²)-----	30.34	(326.6)
Mean aerodynamic chord, m (ft)-----	2.29	(7.5)
Reference center-of-gravity location -----		0.30c
Surface deflection limits, deg:		
Elevator -----		+17, -27
Ailerons -----		+38
Rudders -----		+24
Flaps -----		28

TABLE II.- AERODYNAMIC DATA USED IN SIMULATION

At swath run conditions (1-g trim, V=120 mph, h=3m or 10 ft)

	Basic Aircraft	$\delta_w = 20^\circ$	$\delta_w = -10^\circ$
α	4.31	3.42	3.42
C_L	.637	.636	.636
$C_{L\delta_e}$.00599	.00587	.00587
$\Delta C_{L,ge}$.148	.148	.148
C_D	.0940	.0955	.0955
$\Delta C_{D,\delta_e}$	-.000247	-.000623	-.000623
$\Delta C_{D,ge}$	-.00844	-.00893	-.00893
C_m	.0341	.0397	.0397
$C_{m\delta_e}$	-.0152	-.0150	-.0150
C_{mq}	.230	.230	.230
$\Delta C_{m,ge}$	-.00274	-.00318	-.00318
C_Y	.00172	.00171	.00171
$C_{Y\delta_r}$	-.0061	-.0128	-.0094
$C_{Y\beta}$	-.000569	-.000570	-.000570
$C_{n\delta_r}$.000098	.000157	.000157
$C_{n\delta_a}$	-.00139	-.00128	-.00139
C_{nr}	-.000736	-.000644	-.000638
C_{np}	.000438	.000390	.000459
$C_{n\beta}$	-.00169	-.00190	-.00190
$C_{l\delta_a}$.000171	.000165	.000165
$C_{l\delta_r}$	-.00792	-.00803	-.00792
C_{lp}	.00345	.00608	.00434
C_{lr}	-.00157	-.00449	-.00258
$C_{l\beta}$			

TABLE III.- LATERAL-DIRECTIONAL STABILITY
CHARACTERISTICS IN SWATH RUN

1-g trim, V = 120 mph

CONFIGURATION	P_{DR}	ζ_{DR}	$(\phi/\beta)_{DR}$	τ_R	$(t_{1/2})_S$
Basic	4.34	.246	1.34	.173	68.0
$\delta_w = +20^\circ$	3.54	.201	4.21	.171	10.8
$\delta_w = -10^\circ$	3.96	.223	2.27	.173	19.9

TABLE IV.- THRUST VALUES USED IN SIMULATION

(a) SI UNITS

		Thrust values (N) at a velocity (m/sec) of -								
δ_T	rpm	31	36	40	45	49	54	58	63	67
.1	1000	1047	734	440	106	-249	-604	-959	-1314	-1669
.9	2400	8356	8211	8065	7917	7751	7553	7317	7006	6497

(b) U.S. CUSTOMARY UNITS

		Thrust values (lb) at a velocity (mi/hr) of -								
δ_T	rpm	70	80	90	100	110	120	130	140	150
.1	1000	235	165	99	24	-56	-136	-216	-295	-375
.9	2400	1879	1846	1813	1780	1743	1698	1645	1575	1461

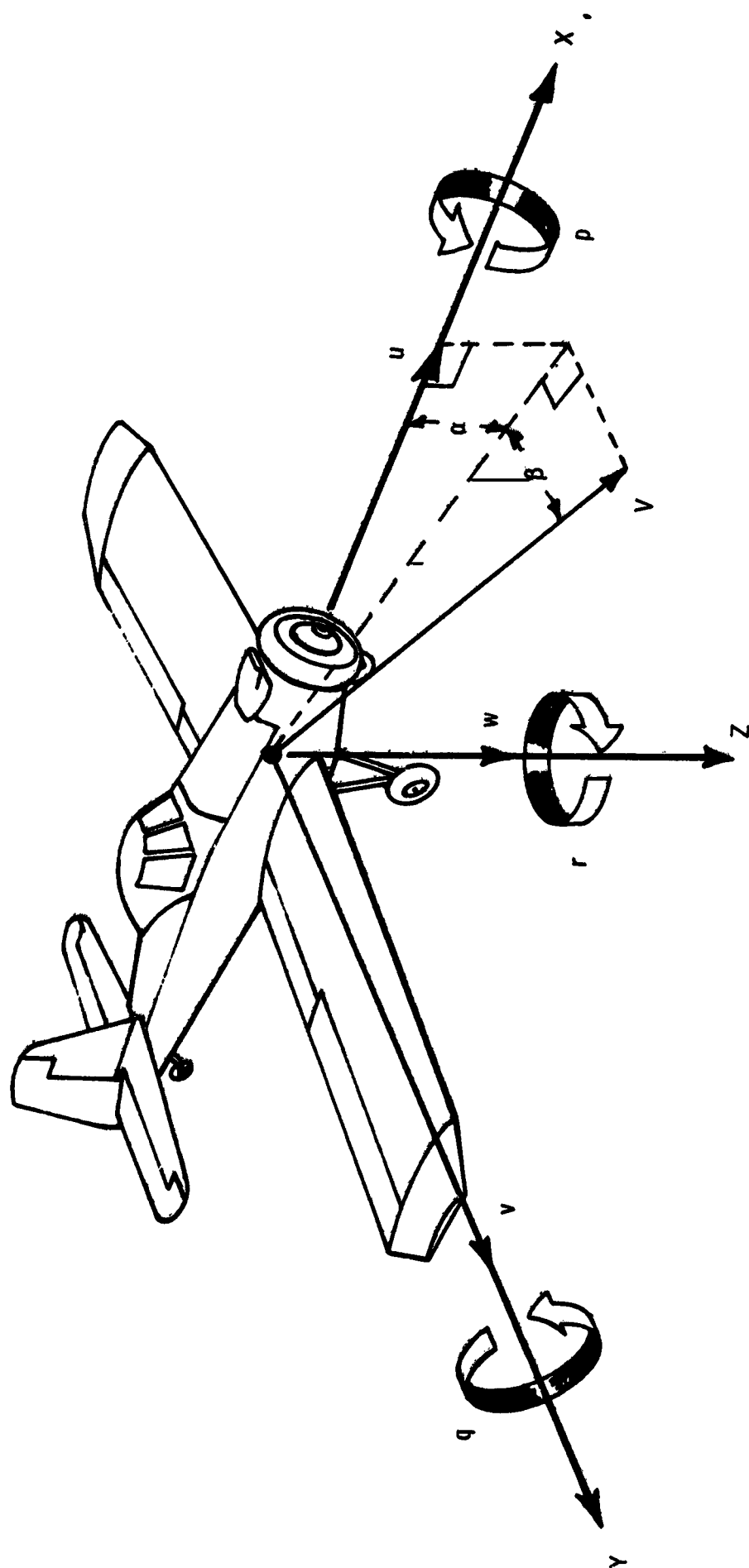


Figure 1. - The body system of axes.

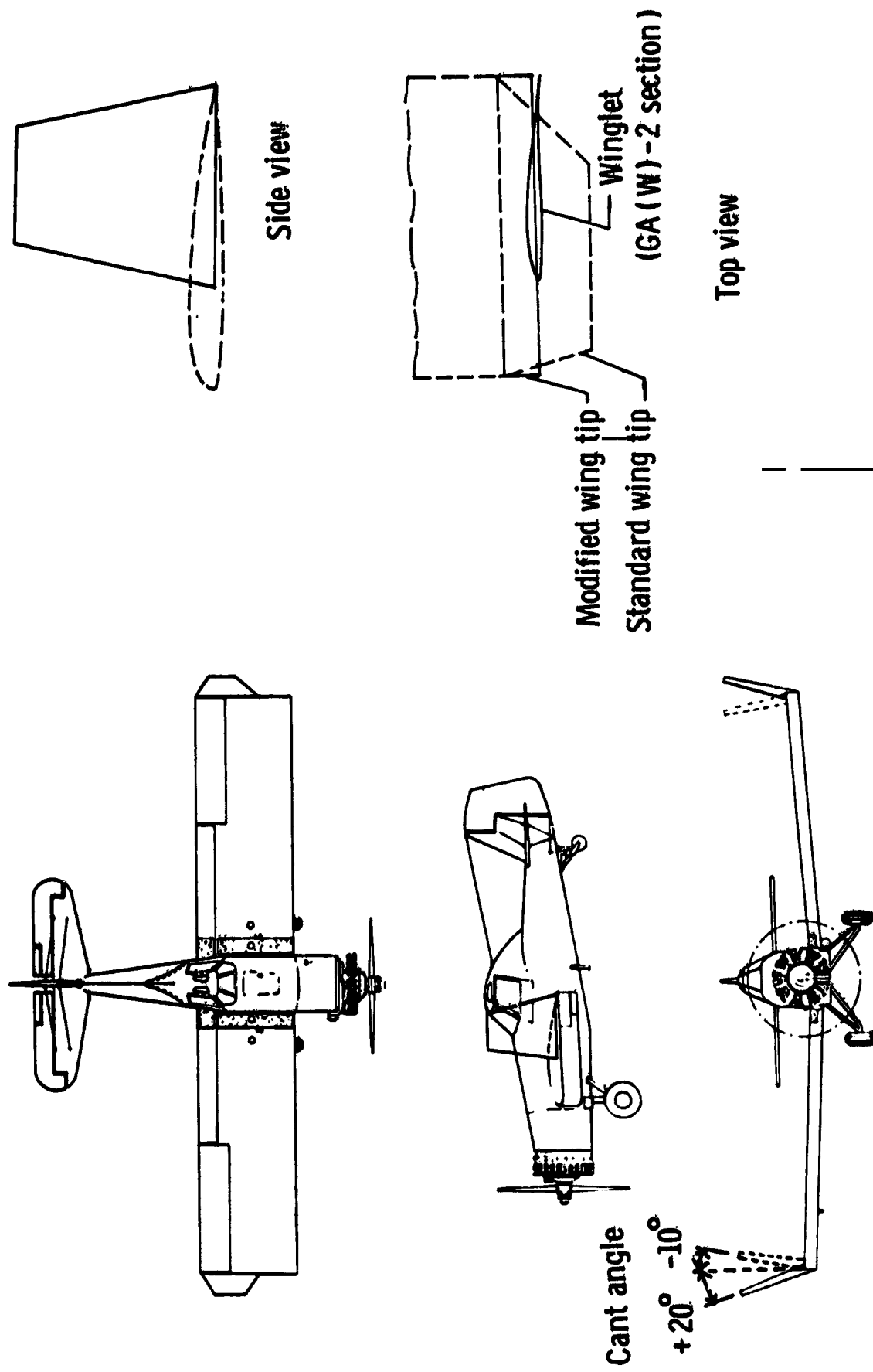


Figure 2. - Three - view sketch of airplane showing winglet installation.

NASA
L-77-5222

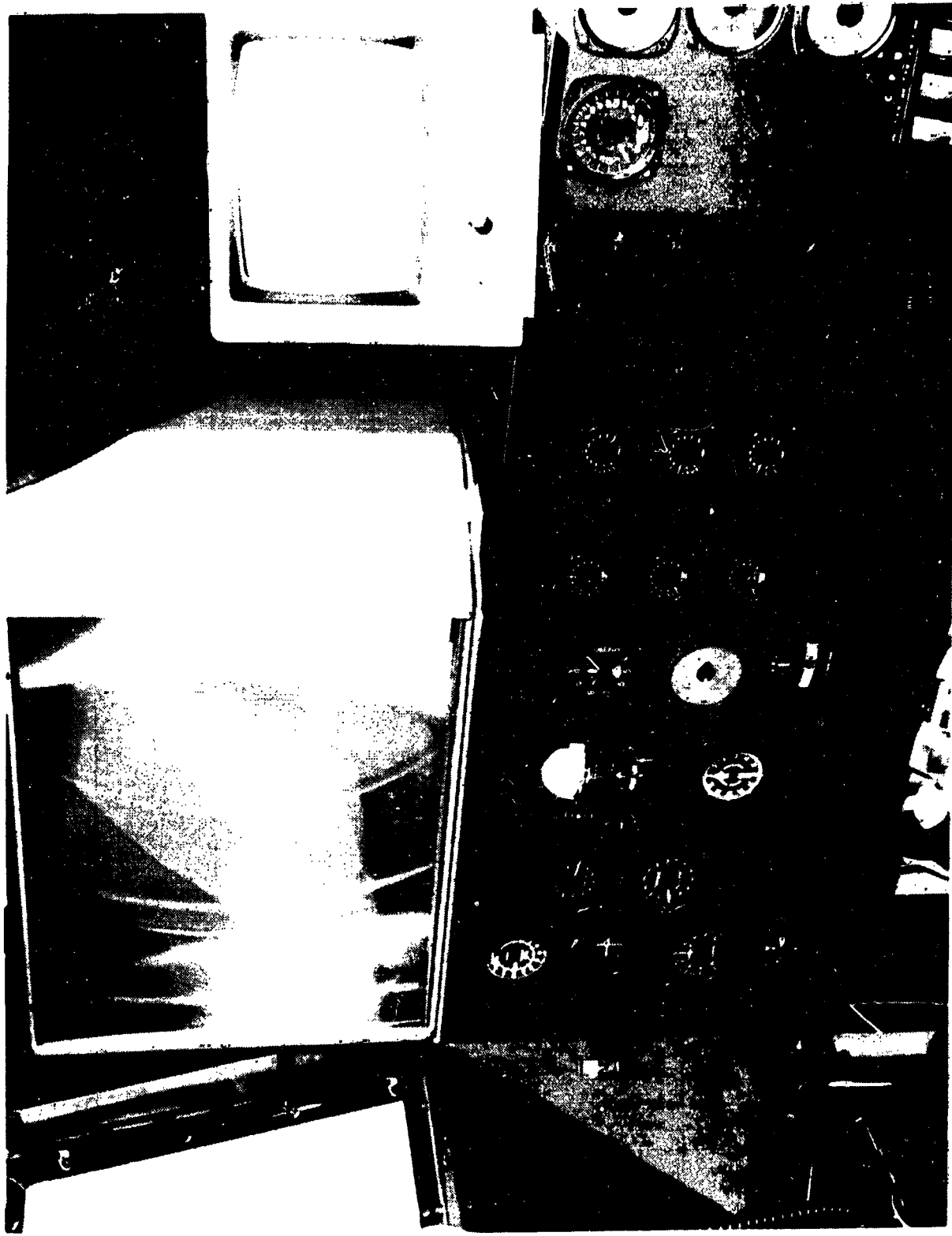


Figure 3. - View of cockpit area of Langley General Purpose Simulator.

<p>CONTROLLABLE</p> <p>Capable of being controlled or managed in context of mission, with available pilot attention.</p>	<p>ACCEPTABLE</p> <p>May have deficiencies which warrant improvement, but adequate for mission.</p>	<p>SATISFACTORY</p> <p>Meets all requirements and expectations; good enough without improvement. Clearly adequate for mission.</p>	1	Excellent, highly desirable.
			2	Good, pleasant, well behaved.
			3	Fair. Some mildly unpleasant characteristics. Good enough for mission without improvement.
	<p>UNSATISFACTORY</p> <p>Reluctantly acceptable. Deficiencies which warrant improvement. Performance adequate for mission with feasible pilot compensation.</p>		4	Some minor but annoying deficiencies. Improvement is requested. Effect on performance is easily compensated for by pilot.
			5	Moderately objectionable deficiencies. Improvement is needed. Reasonable performance requires considerable pilot compensation.
			6	Very objectionable deficiencies. Major improvements are needed. Requires best available pilot compensation to achieve acceptable performance.
	<p>UNACCEPTABLE</p> <p>Deficiencies which require improvement. Inadequate performance for mission even with maximum feasible pilot compensation.</p>		7	Major deficiencies which require improvement for acceptance. Controllable. Performance inadequate for mission, or pilot compensation required for minimum acceptable performance in mission is too high.
			8	Controllable with difficulty. Requires substantial pilot skill and attention to retain control and continue mission.
			9	Marginally controllable in mission. Requires maximum available pilot skill and attention to retain control.
	<p>UNCONTROLLABLE</p> <p>Control will be lost during some portion of mission.</p>		10	Uncontrollable in mission.

Figure 4. - Cooper-Harper handling qualities rating scale.

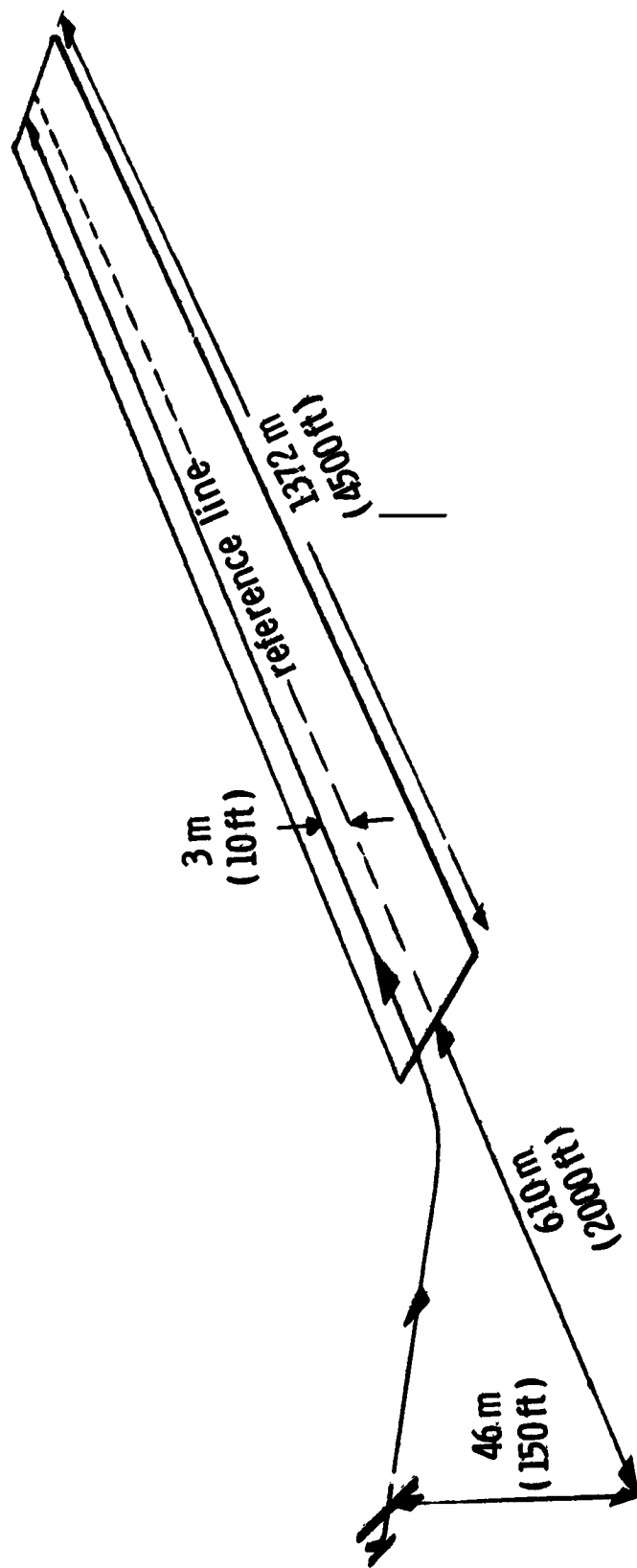


Figure 5. - Sketch of pilot task for handling qualities evaluation.

NASA
1-76-4923

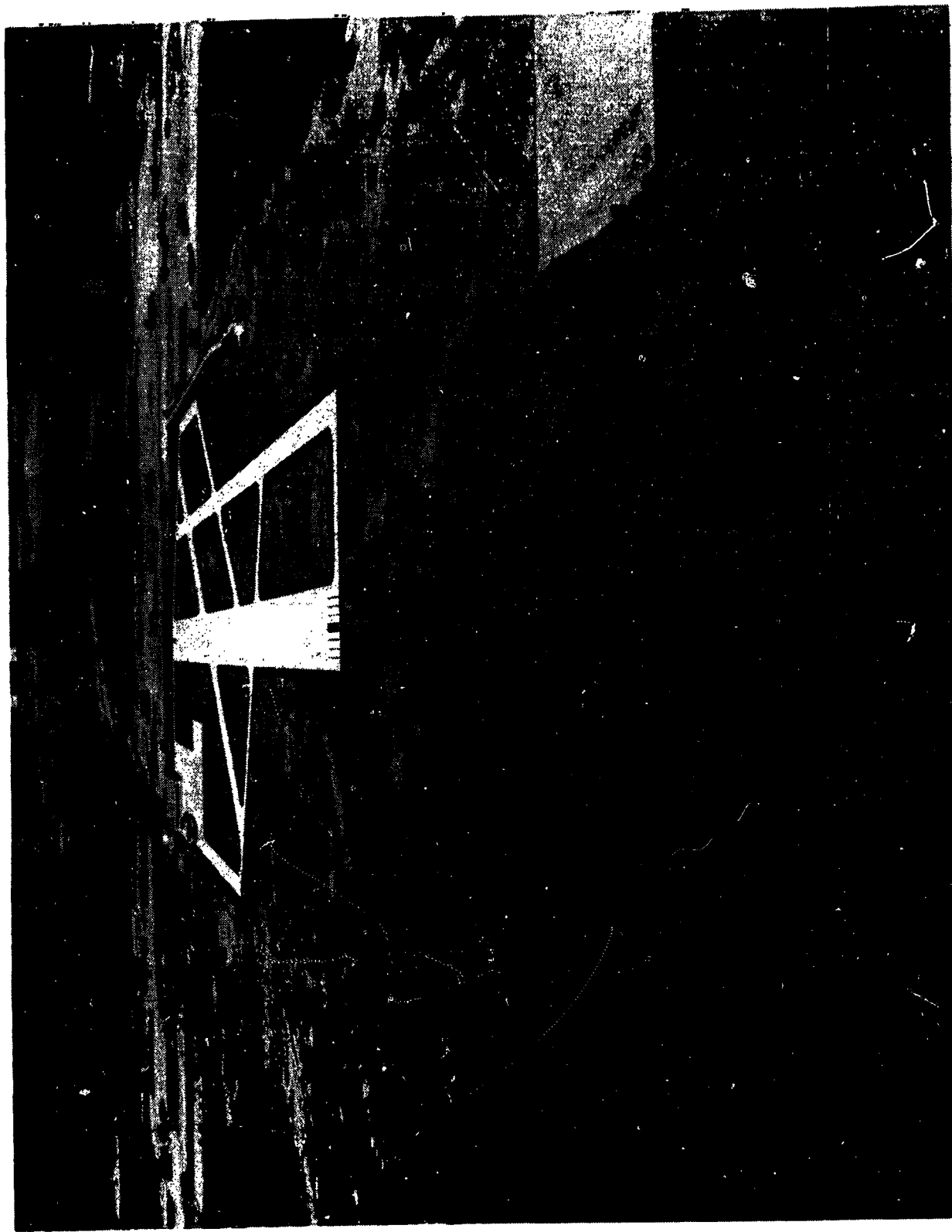
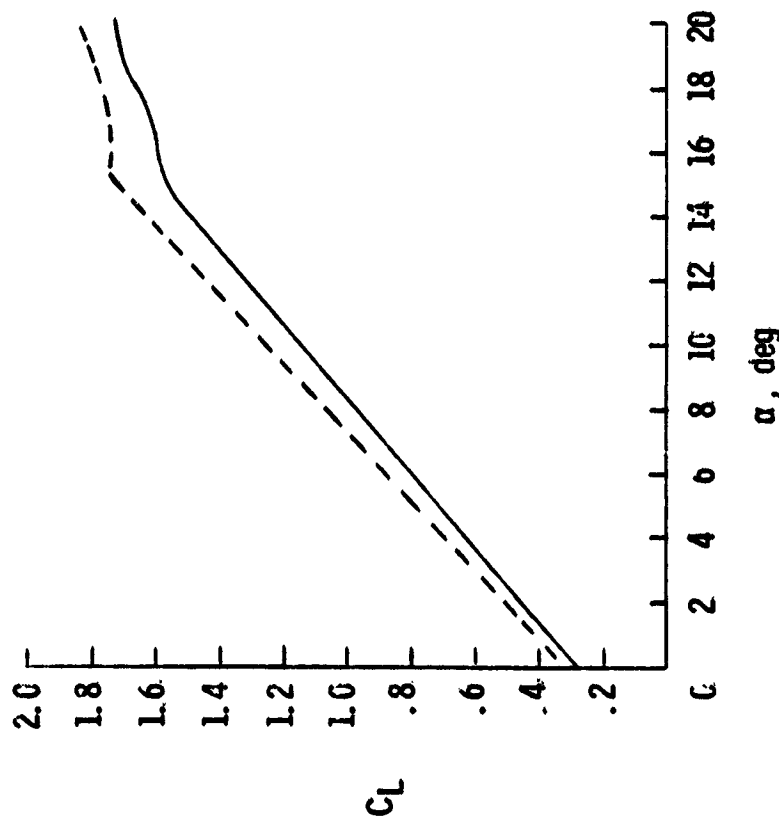
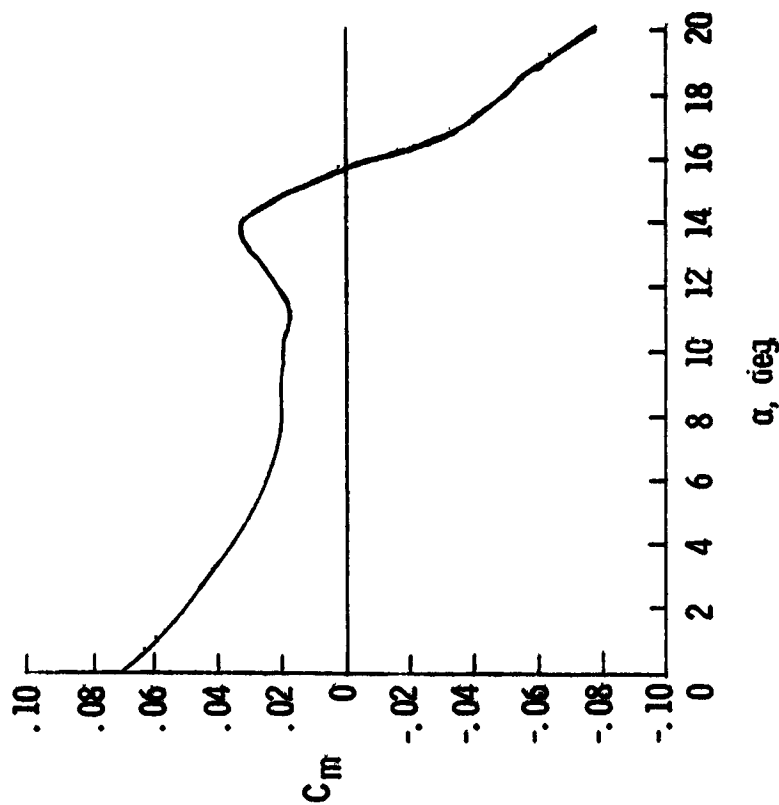


Figure 6. - View of airfield scene generated by VLDS for use
in swath run task

— Basic airplane
 - - - Winglets or, $\delta_w = 20^\circ$ or -10°

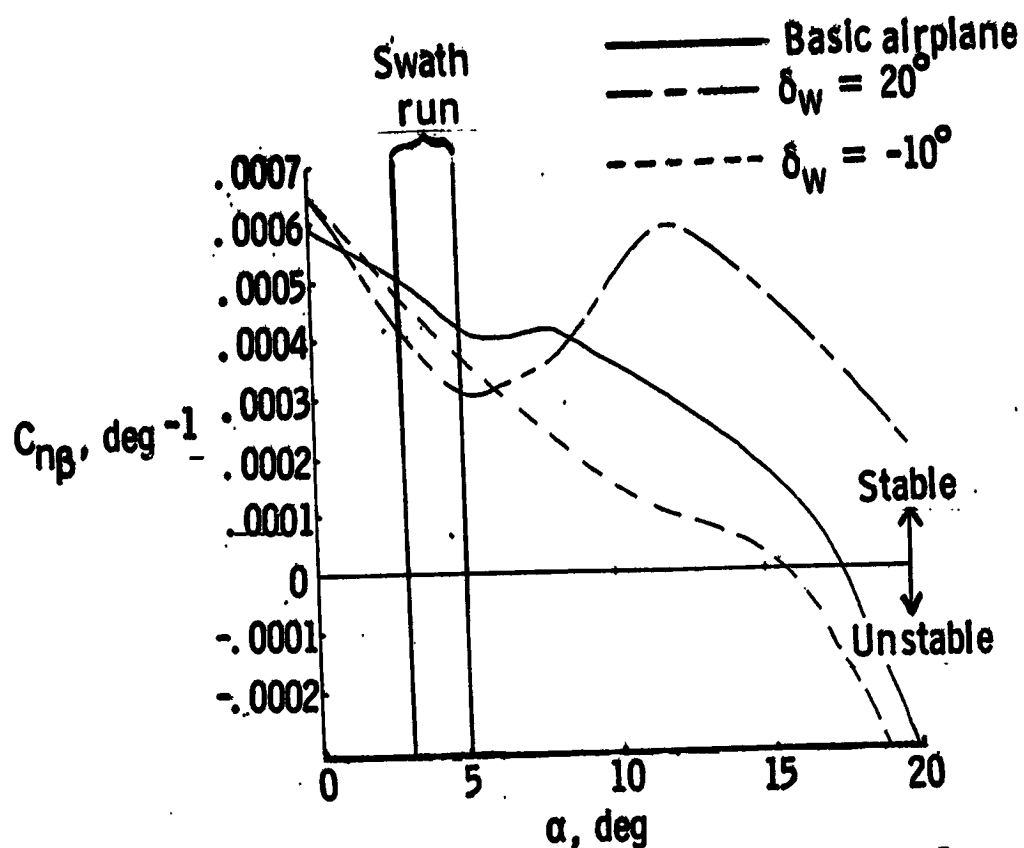


(a) Lift coefficient versus angle of attack.

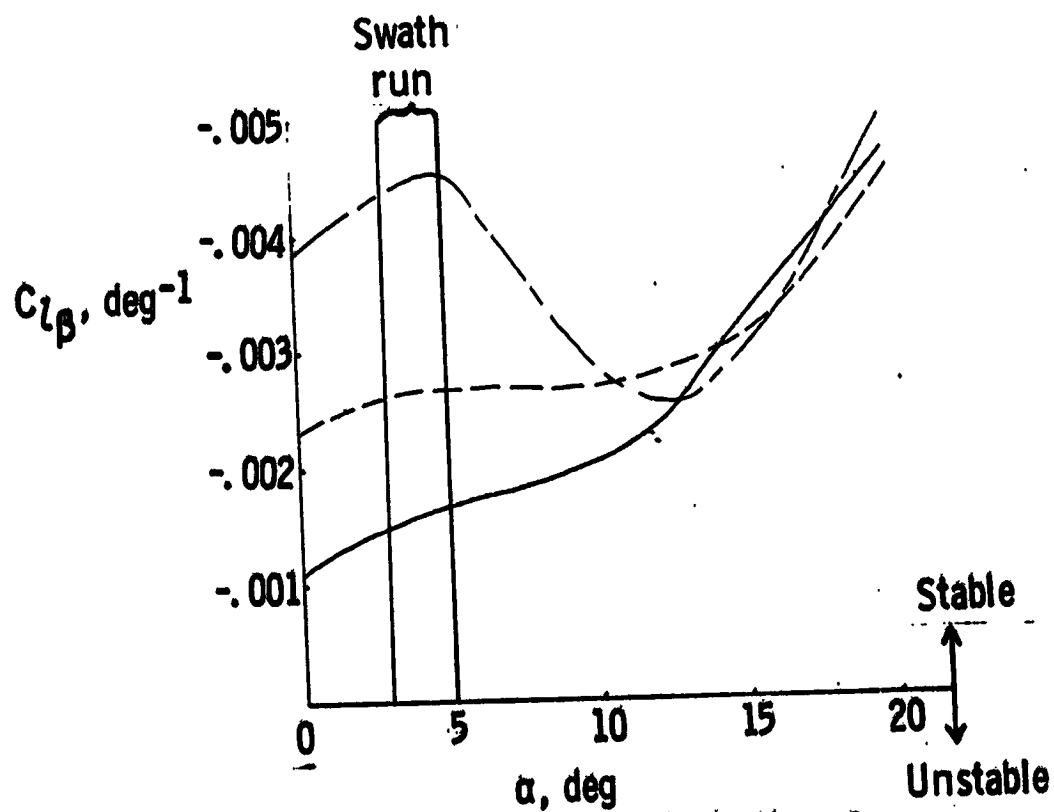


(b) Pitching moment coefficient versus angle of attack
 for airplane with and without winglets.

Figure 7. - Longitudinal characteristics for simulated configuration
 (see reference 2, $C_T = 0.14$).

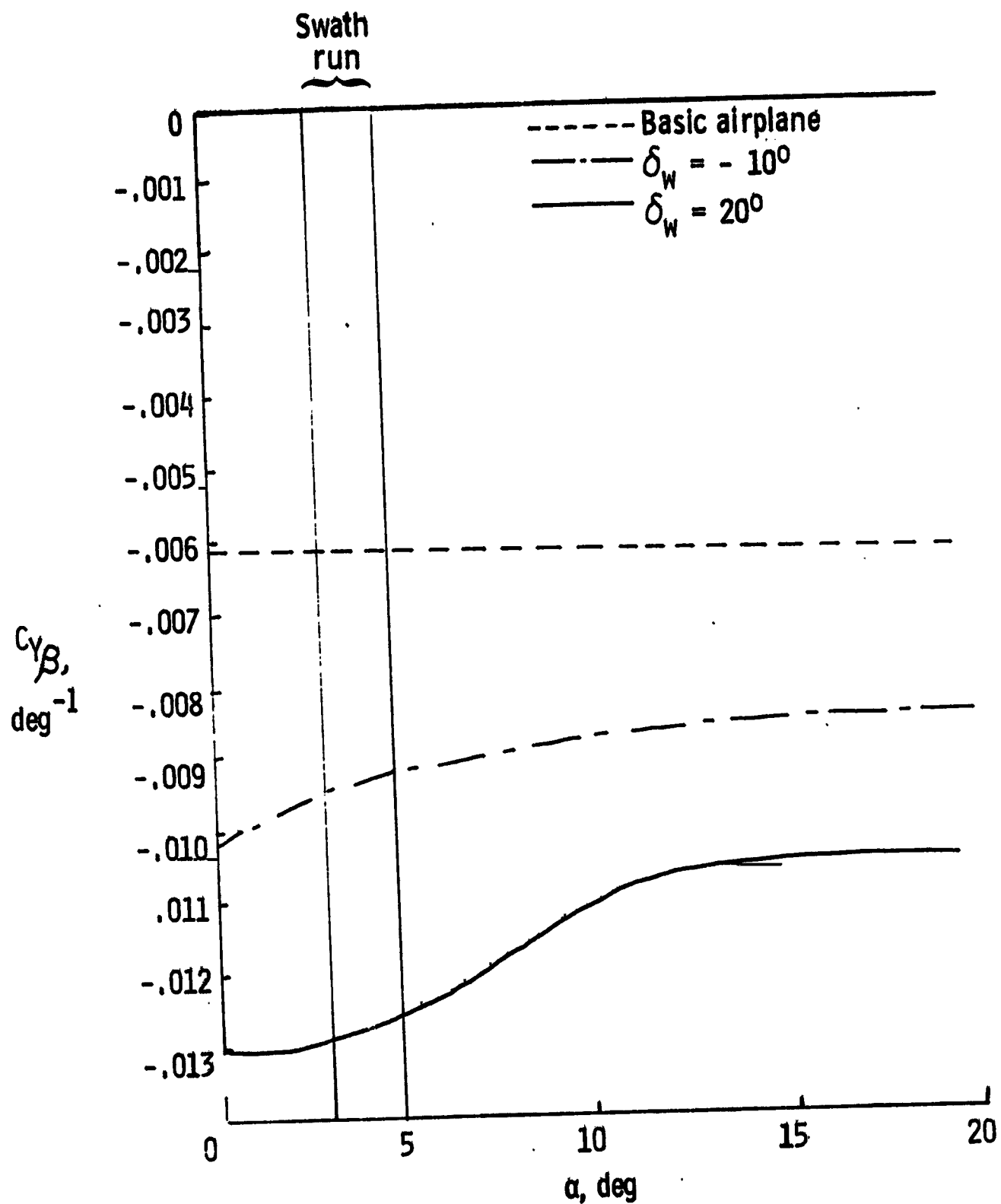


(a) Directional stability derivative, $C_{n\beta}$



(b) Lateral stability derivative, $C_{l\beta}$

Figure 8. - Variation of lateral-directional stability characteristics with angle-of-attack.
($C_T = 0.14$)



(c) Sideforce derivative, $C_{Y\beta}$

Figure 8. - Concluded.

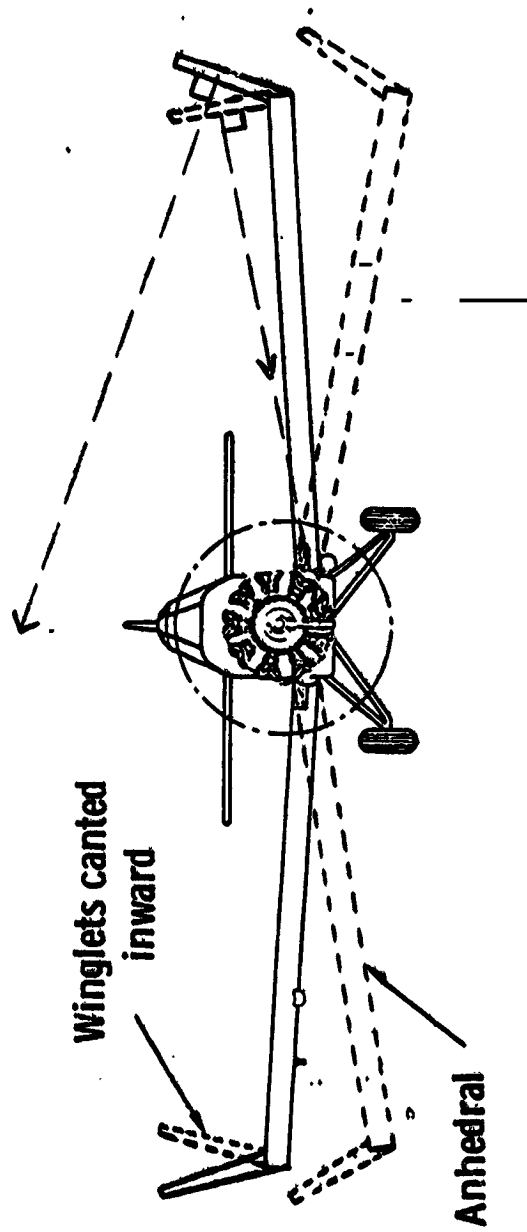


Figure 9. - Two methods for reducing dihedral effect.

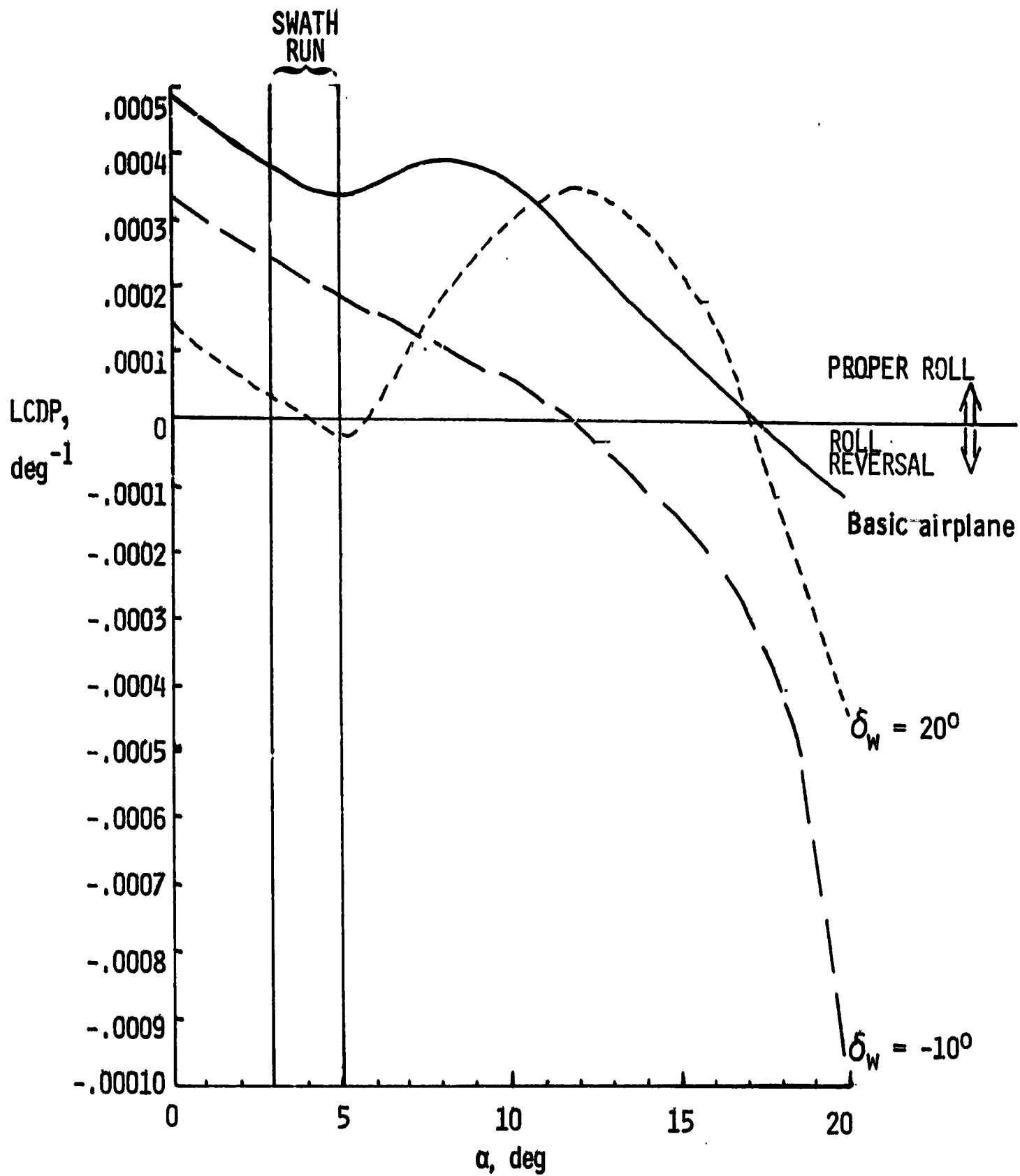


Figure 10. - Variation of lateral control divergence parameter with angle of attack ($C_T = 0.14$).

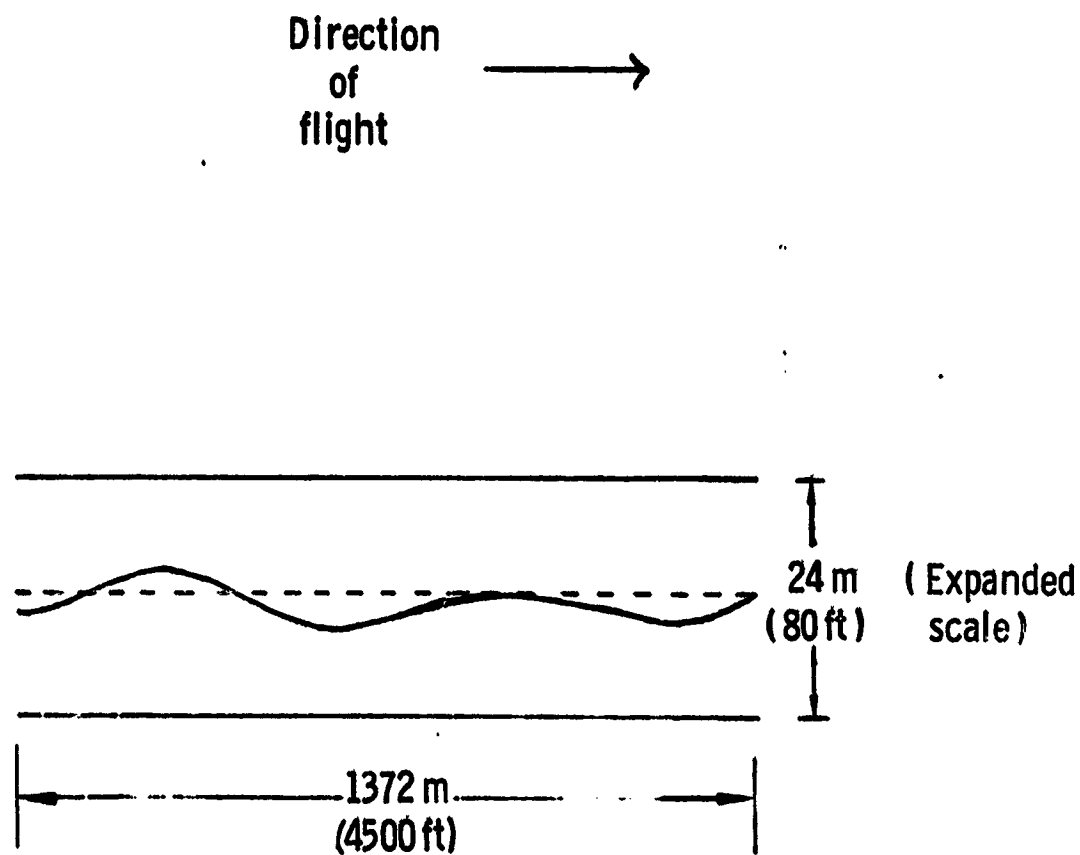


Figure 11. - Ground track showing swath run results for basic airplane.

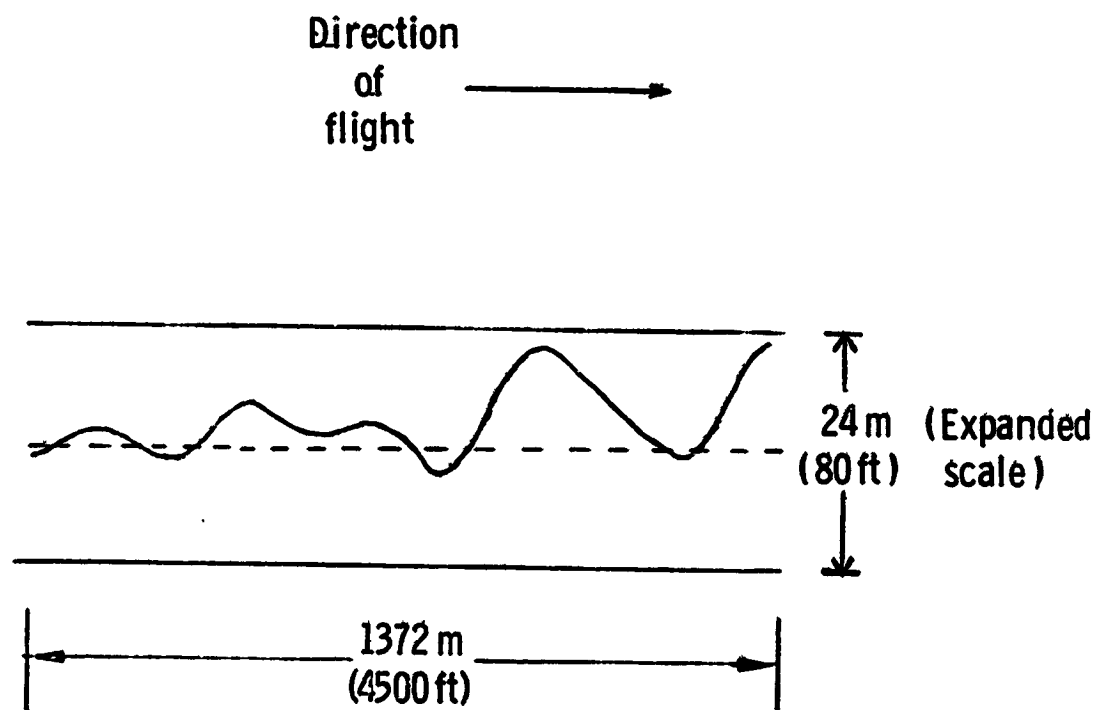


Figure 12. - Ground track showing swath run results for airplane with winglets canted out 20°.

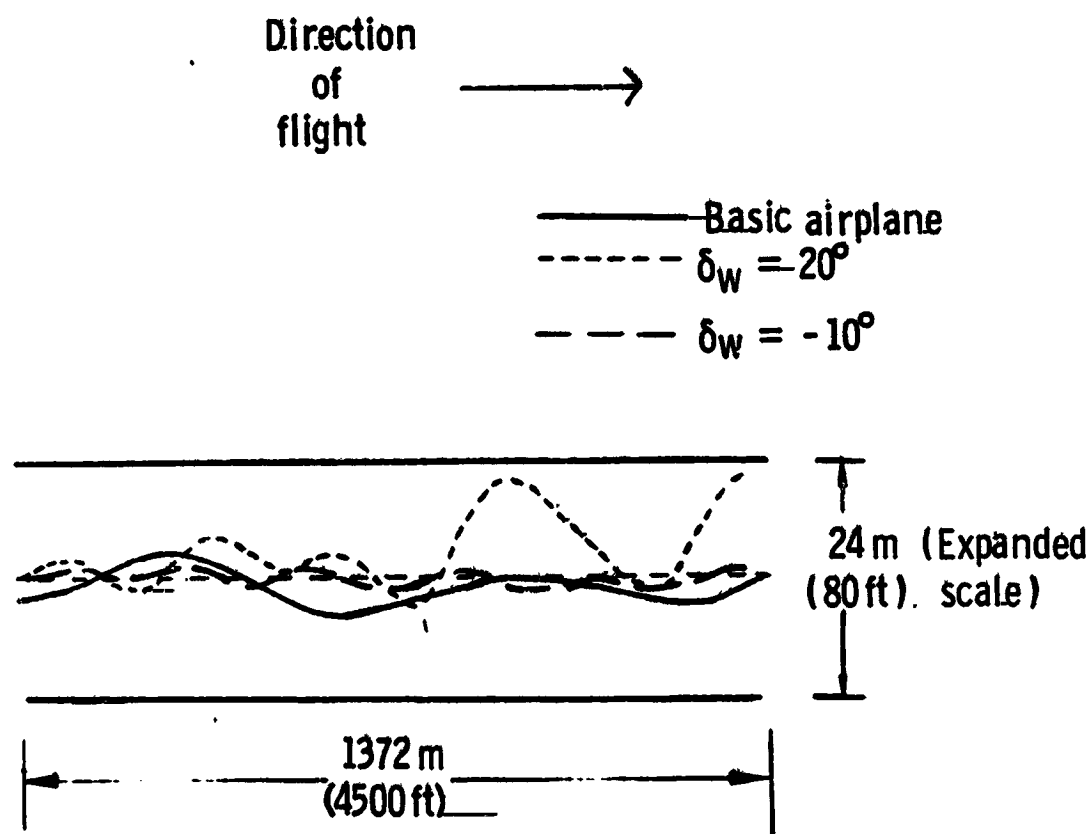


Figure 13. - Ground track showing combined results for three wing - tip configurations.

1. Report No. NASA TM-81817		2. Government Accession No.		3. Recipient's Catalog No.	
4. Title and Subtitle EXPLORATORY PILOTED SIMULATOR STUDY OF THE EFFECTS OF WINGLETS ON HANDLING QUALITIES OF A REPRESENTATIVE AGRICULTURAL AIRPLANE				5. Report Date April 1980	
				6. Performing Organization Code	
7. Author(s) Marilyn E. Ogburn and Philip W. Brown				8. Performing Organization Report No.	
				10. Work Unit No. 505-41-83-01	
9. Performing Organization Name and Address NASA Langley Research Center Hampton, VA 23665				11. Contract or Grant No.	
				13. Type of Report and Period Covered Technical Memorandum	
12. Sponsoring Agency Name and Address National Aeronautics and Space Administration Washington, D.C. 20546				14. Sponsoring Agency Code	
15. Supplementary Notes					
16. Abstract					
<p>An exploratory piloted simulator study has been conducted in order to evaluate the effects on handling qualities of adding winglets to a representative agricultural aircraft configuration during swath-run maneuvering. The aerodynamic data used in the simulation were based on low-speed wind-tunnel tests of a full-scale airplane and a subscale model. The simulation was conducted on the Langley General Purpose Simulator. The Cooper-Harper handling qualities rating scale, supplementary pilot comments and pilot-vehicle performance data were used to describe the handling qualities of the airplane with the different wing-tip configurations.</p> <p>The results of the investigation showed that, for the task evaluated, the lateral-directional handling qualities of the airplane were greatly affected by the application of winglets and winglet cant angle. The airplane with winglets canted out 20° exhibited severely degraded lateral-directional handling qualities in comparison to the basic airplane. When the winglets were canted inward 10°, the flying qualities of the configuration were markedly improved over those of the winglet-canted-out configuration or the basic configuration without winglets, indicating that proper tailoring of the winglet design may afford a potential benefit in the area of handling qualities.</p>					
17. Key Words (Suggested by Author(s)) winglets, dihedral effect, handling qualities, swath run			18. Distribution Statement UNCLASSIFIED - UNLIMITED		
			Subject Category 08		
19. Security Classif. (of this report) UNCLASSIFIED		20. Security Classif. (of this page) UNCLASSIFIED		21. No. of Pages 42	
				22. Price* A03	